



Mapping pine plantations in the southeastern U.S. using structural, spectral, and temporal remote sensing data

M.E. Fagan^{a,*}, D.C. Morton^b, B.D. Cook^b, J. Masek^b, F. Zhao^{c,d}, R.F. Nelson^b, C. Huang^c

^a University of Maryland, Baltimore County, Baltimore, MD 21250, United States of America

^b NASA Goddard Space Flight Center, Greenbelt, MD 20771, United States of America

^c University of Maryland, College Park, MD 20742, United States of America

^d Xi'an University of Science and Technology, Xi'an 710054, China

ARTICLE INFO

Keywords:

Plantations
Lidar
Forestry
Reforestation
G-LiHT
Landsat
Disturbance

ABSTRACT

The southeastern U.S. produces the most industrial roundwood in the U.S. each year, largely from commercial pine plantations. The extent of plantation forests and management dynamics can be difficult to ascertain from periodic forest inventories, yet short-rotation tree plantations also present challenges for remote sensing. Here, we integrated spectral, temporal, and structural information from airborne and satellite platforms to distinguish pine plantations from natural forests and evaluate the contribution from planted forests to regional forest cover in the southeastern U.S. Within flight lines from NASA Goddard's Lidar, Hyperspectral, and Thermal (G-LiHT) Airborne Imager, lidar metrics of forest structure had the highest overall accuracy for pine plantations among single-source classifications (90%), but the combination of spectral and temporal metrics from Landsat generated comparable accuracy (91%). Combined structural, temporal, and spectral information from G-LiHT and Landsat had the highest accuracy for plantations (92%) and natural forests (88%). At a regional scale, classifications using Landsat spectral and temporal metrics had between 74 and 82% mean class accuracy for plantations. Regionally, plantations accounted for 28% of forest cover in the southeastern U.S., a result similar to plot-based estimates, albeit with greater spatial detail. Regional maps of plantation forests differed from existing map products, including the National Land Cover Database. Combining plantation extent in 2011 with Landsat-based forest change data identified strong regional gradients in plantation dynamics since 1985, with distinct spatial patterns of rotation age (east-west) and plantation expansion (interior). Our analysis demonstrates the potential to improve the characterization of dynamic land cover classes, including economically important timber plantations, by integrating diverse remote sensing datasets. Critically, multi-source remote sensing provides an approach to leverage periodic forest inventory data for annual monitoring of managed forest landscapes.

1. Introduction

Growing global demand for wood products, combined with efforts to conserve natural forests, have spurred a 65% increase in the global extent of planted forests since 1990 (FAO, 2015a). Approximately half of all industrial roundwood production in 2012 came from forests established artificially, through either planting or seeding (Payn et al., 2015). The United States is the largest producer of industrial roundwood, accounting for 17% of global production, with an estimated 41% of U.S. production from planted forests that account for only 9% of U.S. forest area (FAO, 2015a; Oswald et al., 2014; Payn et al., 2015; Wear et al., 2016). The majority of U.S. planted forest area (~61%) and wood volume (~57%) is concentrated in industrial pine forest “plantations”

in the southeastern U.S. (FAO, 2015b; Oswald et al., 2014). These intensively managed planted forests are predominantly monocultures of three native pine species (loblolly pine (*P. taeda*), shortleaf pine (*P. echinata*) and slash pine (*P. elliotii*); Oswald et al., 2014).

Despite their importance for global wood production, pine plantations in the southeastern U.S. are not well characterized in terms of their total area, spatial arrangement, or management dynamics (Zhang and Polyakov, 2010). Recent studies suggest that pine plantations are expanding in the region and replacing both natural forests and non-forest habitats (Hanberry, 2013; Wear and Greis, 2013), with natural forest conversion to plantations estimated at 0.45% per year between 1989 and 1999 (Wear and Greis, 2002). Current estimates of plantation area are largely derived from U.S. Forest Inventory and Analysis (FIA)

* Corresponding author.

E-mail address: mfagan@umbc.edu (M.E. Fagan).

<https://doi.org/10.1016/j.rse.2018.07.007>

Received 11 January 2018; Received in revised form 30 June 2018; Accepted 4 July 2018

0034-4257/ © 2018 Elsevier Inc. All rights reserved.

plots (Oswalt et al., 2014; Pan et al., 2011; Wear and Greis, 2013; Zhang and Polyakov, 2010). With uniform sampling methods since the year 2000, FIA data provide robust estimates of planted forests at large scales (county or state administrative units; O'Connell et al., 2015; Schroeder et al., 2014; Wear and Greis, 2002; Zhang and Polyakov, 2010). However, FIA plots sample a small proportion of the landscape (0.6 ha per 2428 ha; O'Connell et al., 2015), reducing their utility for characterizing fine scale (1–100 ha) land use patterns or lower frequency events such as forest disturbances, natural regeneration on abandoned lands, and plantation expansion (Boisvenue et al., 2016; Czaplowski, 2010; Schleeweis et al., 2013; Schroeder et al., 2014; Williams et al., 2014).

By contrast, satellite remote sensing data provide complete spatial coverage at spatial resolutions consistent with plantation forest management, yet dynamic plantation landscapes remain a challenge for traditional land cover classification or forest change products. National and regional land cover maps do not isolate tree plantations as a map class (Hansen et al., 2013; Masek et al., 2013; Ruefenacht et al., 2008; Xian et al., 2009; Yeo and Huang, 2013, but see Drummond et al., 2015). Previous remote sensing studies in the southeastern U.S. have characterized forest change without attribution to planted or natural forest types (Hansen et al., 2013; Jin et al., 2013; Masek et al., 2013). In addition to timber harvests, management of pine plantations through thinning, burning, or herbicidal treatments may be detected as forest change at Landsat resolution (Cohen et al., 2016; Harris et al., 2016; Masek et al., 2013; Schleeweis et al., 2013). A number of studies have used optical or lidar remote sensing to characterize pine plantations across small areas (Banskota et al., 2011; Blinn et al., 2012; Petersen et al., 2016; Popescu et al., 2004; Shamsoddini et al., 2013; Van Aardt and Wynne, 2007). However, relying on a single type of remotely-sensed data can limit the ability to isolate tree plantations, especially for native tree species that are spectrally and structurally similar to natural vegetation (Drummond et al., 2015; Fagan et al., 2015; Puyravaud et al., 2010). The potential to overcome these limitations by integrating different data types has not been extensively explored for mapping tree plantations. Classifications of “tree crops” (tree plantations for crop production) such as rubber and oil palm have benefitted from optical-SAR fusion (Chen et al., 2016; Dong et al., 2013; Gutiérrez-Vélez and DeFries, 2013; Joshi et al., 2016; Qin et al., 2016; Torbick et al., 2016), but timber plantations often have greater structural resemblance to natural forests than tree crop plantations (Brockerhoff et al., 2008).

Tree plantations have several distinct spectral, structural, and temporal characteristics that may increase the likelihood of detection using a diversity of remote sensing data types. First, most plantations established for wood production are single-species monocultures, which leads to spectral homogeneity at spatial scales consistent with moderate resolution (30 m) multispectral and hyperspectral imagery (Danson and Curran, 1993; van Aardt and Norris-Rogers, 2008). Second, even-aged monoculture stands tend to have homogenous canopy structure, which could be detected using very high resolution imagery (Shamsoddini et al., 2013), lidar, or radar (e.g., Dong et al., 2013; Donoghue et al., 2007). Finally, the temporal signal of regular stand harvesting and replanting may be discernable using long time series of passive or active remote sensing data (le Maire et al., 2014). Algorithms to detect annual or subannual forest disturbance and regrowth in moderate-resolution optical data (e.g., Cohen et al., 2017) provide estimates of forest cover change since 1984 using Landsat data. In the southeastern U.S., timber harvests are common in both natural forests and pine plantations, but intensive management in pine plantations typically results in shorter harvest rotations than natural pine and mixed deciduous forests (Smith et al., 2006; Wear and Greis, 2002; Zhou et al., 2013).

In this study, we quantified the extent of plantations in the southeastern U.S. using structural, spectral, and temporal data from airborne and satellite remote sensing platforms. Specifically, we evaluated the ability of three main types of remote sensing data, alone and in

combination, to distinguish pine plantations from natural forests of mixed pine and deciduous species. Along flight lines of NASA Goddard's Lidar, Hyperspectral, and Thermal (G-LiHT) Airborne Imager, we first assessed (1) structural data from small footprint lidar, (2) spectral data from Landsat NDVI, lidar apparent reflectance, and national land-cover classifications derived from Landsat imagery, and (3) temporal data on forest disturbance derived from Landsat time series. We hypothesized that structural or temporal data alone would each be more effective than spectral data for distinguishing pine plantations, given variability within and among plantations based on the diversity of age classes, management impacts (e.g., thinning), and species composition (Wear and Greis, 2002). Second, after evaluating methods for mapping plantation forests using only spectral and temporal metrics from Landsat, we estimated the regional extent of plantation forests and harvest dynamics. Regional maps of plantation forests are critical for quantifying spatiotemporal differences in forest management and the impacts of plantation forests on habitat connectivity, landscape fragmentation, and the contribution from forest management to U.S. forest carbon sources and sinks (Coulston et al., 2015; Wear and Greis, 2013; Zhou et al., 2013).

2. Methods

2.1. Study area and system

The study region encompassed two large ecoregions (Olson et al., 2001), the southeastern mixed forests and the middle Atlantic coastal forests (Fig. 1), and covered most of the coastal plains and piedmont of the southeastern U.S. where industrial pine forests are common. Pine plantation monocultures in the study region originate either through direct planting, direct seeding, or natural regeneration followed by herbicidal removal of competing deciduous species. Thinning of timber stands is common, either through selective felling or direct removal of young trees in rows. Upland natural habitat in this landscape is dominated by mixed conifer-deciduous forests, with occasional stands of longleaf pine on sandy soil, and riparian habitats are dominated by deciduous bottomland forests.

2.2. Data sources

2.2.1. Structural data

Lidar data were collected in June–August of 2011 by NASA's G-LiHT Airborne Imager (Nelson et al., 2017). The G-LiHT lidar uses a 1550 nm wavelength, with 5–10 pulses/m² and a maximum of 4 returns per pulse (Cook et al., 2013). Lidar data were restricted to the central 30° field of view. A total of twelve flight lines fall within the study region (Fig. 1), totaling ~81,000 ha (2700 km × 0.3 km; Nelson et al., 2017). G-LiHT data are available online at <https://gliht.gsfc.nasa.gov/>.

G-LiHT lidar data were used to characterize vegetation structure in tree plantations, natural forests, and open habitats along the flight lines. We calculated standard lidar metrics at 15-m resolution to be consistent with both the 7.3 m radius of FIA sub-plots and 30 m Landsat data. Three novel metrics that characterized spatial variability in the vertical profile of lidar returns are described in more detail in the Supplementary materials. A total of 24 metrics (Table S1) were used to capture structural attributes of plantation forests and other vegetation after eliminating highly correlated metrics ($r > 0.9$).

2.2.2. Spectral data

We used three main sources of spectral data to discriminate plantation forests, natural forests, and non-forest land cover classes. First, to characterize the phenology of evergreen and deciduous vegetation, we calculated seasonal NDVI metrics from Landsat 5 composites in Google Earth Engine. Cloud- and snow-free spectral composites for 2011 were created using median pixel values of all available imagery for summer (June–August) and winter (November–February). Seasonal metrics

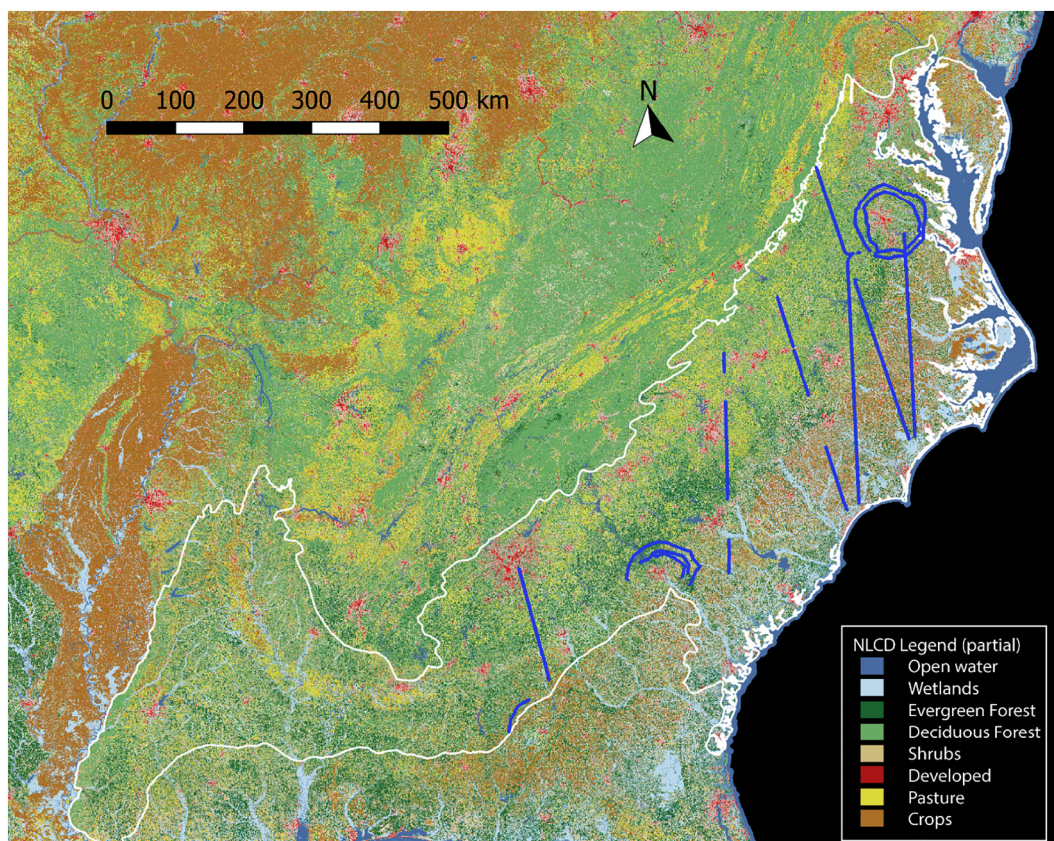


Fig. 1. A map of the southeastern U.S., delimiting the study region (white lines) and the G-LiHT lidar flight lines (dark blue lines). The map shown is the 2011 National Land Cover Database (NLCD; see the full legend at https://www.mrlc.gov/nlcd11_leg.php). (For interpretation of the references to colour in this figure legend, the reader is referred to the web version of this article.)

included winter NDVI, summer NDVI, the difference between winter and summer NDVI, and standard deviation in NDVI metrics (3×3 window; Table S1). Second, the National Land Cover Database (NLCD, Homer et al., 2015) land cover map for 2011 was reclassified into eight main land cover types, including five forest types (Table S2). Third, lidar apparent reflectance (1550 nm) was calculated using instrument-calibrated, range corrected reflectance values for single return laser shots (Cook et al., 2013; Pfennigbauer and Ullrich, 2010). We calculated summary metrics of lidar apparent reflectance at 15 m resolution (see Table S1). Lidar reflectance data were available only along the G-LiHT flight lines, while the Landsat-derived spectral data extended across the entire study area.

2.2.3. Temporal data

We used two sources of Landsat-derived data on forest disturbance, the Hansen et al. (2013) global forest change dataset (HGFC; 2000–2011) and the Vegetation Change Tracker dataset (VCT; 1985–2011) developed by the North American Forest Dynamics (NAFD) study (Huang et al., 2010; Masek et al., 2013; Zhao et al., 2018). From the HGFC dataset, we used annual products of forest gain and year of loss. We calculated several additional temporal metrics from the annual VCT dataset describing forest dynamics, including the age of forest regrowth (reforestation), the total number of disturbances, the occurrence of regrowth after recent disturbance, the disturbance of existing regrowth, and the time elapsed as nonforest between disturbance and regrowth (Table S1; see Supplementary materials). The VCT algorithm identifies regrowth when it reaches a stage where the regrowing trees are spectrally similar to a forest; in our processing of the VCT data, a regrowth event refers to this point in time, when a pixel transitions from nonforest to forest cover. In this paper, we refer frequently to the HGFC forest gain product (“HGFC gain”) and the VCT reforestation age

(“VCT forest age”).

2.3. Land use classification

2.3.1. Development of training and testing data along lidar flight lines

A sample of 21 lidar flight line segments was randomly selected from the 420–7 km segments of G-LiHT data in the study region for training and validation of land use classification products. Land cover patches ≥ 2 ha within each flight line segment were assigned to one of three land cover types using high-resolution image time series available in Google Earth: pine plantations, natural forests, and open (non-forest) cover types (see Supplementary materials for details). Where image time series were unavailable, data were cross-checked in the corresponding GeoEye or DigitalGlobe data (Neigh et al., 2013).

2.3.2. Classification along lidar flight lines

Within G-LiHT lidar flight lines, structural, spectral, and temporal metrics were used alone and in combination to discriminate tree plantations from other land uses (Fig. 2). Landsat-based spectral and temporal data were resampled (nearest neighbor) to the 15 m grid resolution used for lidar structural metrics. Training and testing data for all classification models were created by dividing the reference data in each flight line segment randomly into two groups (North and South, separated by a 150 m buffer in the middle), with one half randomly assigned to training data and the other to testing data. Testing data locations were then randomly subsampled (100 pixels per flight segment; 4.7% of the total number of pixels within testing polygons) to decrease the influence of spatial autocorrelation within testing polygons.

For each combination of input data, we developed a decision tree model (CART: Breiman et al., 1984) to classify the data and analyze

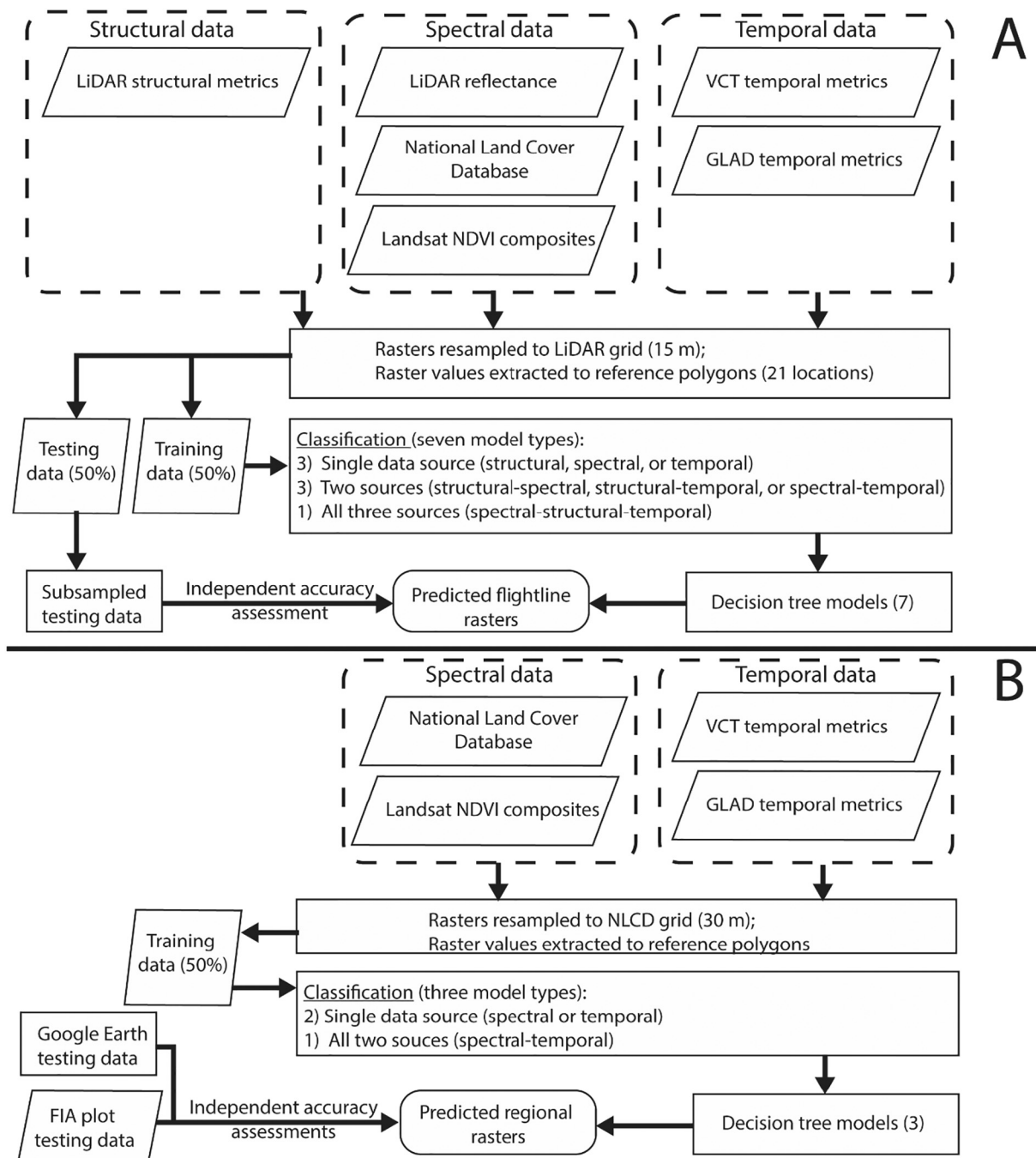


Fig. 2. A diagram of the workflow in this study. Part A shows the analysis focused on the G-LiHT flight lines, and Part B shows the regional analysis with Landsat-derived data.

specific variable contributions. Decision tree models were created with default parameters and a uniform pruning criterion ($\alpha = 0.002$). All classification analyses were conducted in R 3.02 (R Core Team, 2013) using the rpart package (Therneau et al., 2015).

2.3.3. Regional land use classification and accuracy assessment

A second land use classification for the broader southeastern region was developed using only the Landsat-derived spectral and temporal metrics (Fig. 2). Training data for the regional classification models was derived from the flight line land use polygons described above. For the regional classification, three combinations of input data were used to develop classification models: spectral, temporal, and combined temporal and spectral data. The predicted regional, three-class map was

sieved; clusters with < 25 contiguous pixels were reclassified using the majority land cover of neighboring pixels (GDAL sieve algorithm, queen connectivity). This 2.25 ha minimum mapping unit improved overall map accuracy by decreasing speckle within plantations and natural forests (Tables S3, S4).

Regional map accuracy was assessed using two independent sets derived from FIA field plots ($n = 2938$) and Google Earth imagery ($n = 300$), with a post-stratified estimator (Olofsson et al., 2013). Pine plantations were identified in the database of FIA field plots based on the dominant species, age < 50 years, and stand origin status as planting or artificial seeding. The FIA stand origin definition thus excludes industrial forests created through herbicide and thinning of naturally regenerating pine stands. We assessed model predictions (in

0.81 ha plots) against all FIA field plots (0.6 ha) from 2010 to 2012 (see Supplementary for details). To correct for potential inconsistencies in the definition of planted forest between FIA data and our training data, an additional 300 testing data locations (0.81 ha) were randomly located across the region. At each location, the full available time series of high-resolution imagery in Google Earth was used to identify conifer monocultures under intensive plantation management.

We also assessed the accuracy of existing land cover maps using a similar methodology. We evaluated four products, including NLCD land cover, VCT forest age, and HGFC forest gain, along with a composite map (“NLCD-VCT-HGFC”) to see if it was possible to map plantations by simply selecting key forest types that were recently disturbed. The composite map predicted plantations where NLCD evergreen and shrub forests classes were classified as regrowth in either the VCT or HGFC maps. The performance of these land cover maps was assessed using the flightline reference data (training and testing) and independent FIA and Google Earth validation data.

2.4. Forest dynamics analysis

Spatial patterns in tree plantation expansion, disturbance frequency, and rotation rates were analyzed by combining the regional classification of pine plantations in 2011 with VCT forest change data from 1985 to 2011. Plantation expansion was identified based on the establishment of pine plantations following ≥ 8 years of consecutive nonforest classification, to avoid counting reforestation after harvesting as expansion (see Supplementary materials). Disturbance frequency for areas classified as pine plantations in 2011 was estimated by tallying observed disturbance events in the VCT time series. Rotation age was calculated for pine plantation areas in 2011 with a history of one regrowth event followed by a disturbance event (pixels without both regrowth and disturbance events were not included in rotation age calculations). To analyze regional differences in disturbance rates, expansion area, and rotation age, pixels were aggregated to 5 km grid cells, and second-order trend surfaces were fit to test for general spatial trends. At the local scale, clustering in the expansion of pine plantations was analyzed based on edge-to-edge distance between expansion areas and existing plantation forests.

To further characterize rates of plantation regrowth across the region, the consistency between estimated plantation age (VCT) and lidar-derived tree height (mean CHM height) was assessed along G-LiHT flight lines. The height-filtering methodology described by Neigh et al. (2016) was used to correct for scale-mismatches between lidar-measured individual tree heights and VCT-derived clearing age (i.e., seed trees left behind after clearing events).

3. Results

3.1. Classification with structural, spectral, and temporal data

Overall accuracy for the flight-line classifications was $> 85\%$ for every model (Fig. 3; Table S3). The all-data model had the highest overall accuracy (92.1%), but results from the two-source models were comparable (91.1–92.0%). Forest classes were readily distinguishable from nonforest using only one data source—structural, spectral, or temporal data (Table S3).

Mean class accuracy for tree plantations varied more among models (Fig. 3). In the flight line classification, lidar-derived structural metrics best discriminated tree plantations from other forest types, with 79.6% mean class accuracy (Fig. 3). Classification accuracy of pine plantations improved with the addition of the other data types (83.1% mean class accuracy for all-data model; Fig. 3). However, the pairwise combination of spectral and temporal data had the highest mean class accuracy (85.8%) for distinguishing tree plantations within G-LiHT flight lines.

The best overall decision tree model for flight line classification highlighted the relative contributions from structural, temporal, and

spectral data. Structural data on canopy height variability were selected in the top two decision tree splits, first dividing the data into forest/nonforest and then separating short forests from medium and tall forests (Fig. S1). Further divisions were made using all three data sources, with important contributions from spectral data (NLCD, lidar reflectance). In general, temporal data were less important than spectral and structural data, but three temporal metrics were among the top ten most important variables in the all-data model (presence of regrowth, regrowth age, and time between disturbance and regrowth). Data types differed in their ability to distinguish land uses, and the top 15 variables in the all-data model were not equivalent to the top 5 variables for the three single data-source models (Table S4). Four of the five most important variables were structural, providing further support that structural data were best suited to distinguish among all three land use classes. Structural variables that clearly distinguished between natural forest and plantations include several metrics of canopy variability (e.g., standard deviation of return height), fractional cover, and the percentage of returns that reached the ground (10th percentile; see Fig. S1). Mean return height, a common metric for modeling forest biomass, was not used for classification due to high correlation ($r = 0.9$) with other lidar metrics.

Plantation tree height within the lidar coverage increased as a function of Landsat-derived stand age (Fig. 4; power law fit, $p < 0.0001$, $r^2 = 0.72$). The plantation site index (i.e., expected stand height at a given age) estimated along the lidar flight lines had a mean prediction of 17.1 m at 25 years, with a 95% confidence interval between 10 and 29.5 m (Fig. 4). Across a number of timber production field plots, plantation site index ranged from 12 to 30 m at 25 years (median of 18 m; Sabatia and Burkhart, 2014). In our study, growth rate filtering decreased the variance of the estimated growth rates, but not the overall shape of the best fit trendline. The high variability in the height-age relationship is to be expected from both methodological issues (e.g., time lags for the detection of regrowth in imagery, missed disturbance events, seed tree silviculture), and differences in site conditions and management that influence productivity across the region.

3.2. Regional classification with spectral and temporal data

Overall, regional classification models created using only Landsat-derived spectral and temporal metrics had lower accuracy than the classification models created with all three data sources within G-LiHT flight lines (Fig. 3). The combined spectral-temporal data model had the highest overall classification accuracy among the regional models (88.3% overall accuracy, LSPEC-TEMP; Fig. 3). The spectral-temporal model classified tree plantations with 77.8% mean class accuracy (Fig. 3, Table S3), and post-classification filtering of clusters < 2.25 ha further improved mean tree plantation class accuracy to 82.2% (Table S5). Both spectral and temporal metrics contributed to the best combined model. NLCD forest type was the first split, separating the dataset into forest and nonforest. Subsequent splits in the decision tree accounted for the presence of regrowth, before forest age, NLCD type, and NDVI thresholds were selected to separate regrowth into plantation and natural forests, and to a lesser extent, separate natural forest from older (non-regrowth) plantations (Fig. S2).

An independent, post-stratified accuracy assessment using Google Earth imagery of the filtered best regional land-use map was comparable to accuracy using the flightline testing data, with 92.6% overall accuracy and 81.8% mean class accuracy for plantations (Tables 1B, S6B). Independent post-stratified FIA estimates of mean class accuracies for the filtered map were lower ($n = 5404$; Tables 1A, S6A; 85.2% for natural forests and 73.6% for tree plantations). When restricted to FIA plots in conifer-dominated forests < 50 years in age, the ability of the classifier to distinguish natural forests from tree plantations decreased dramatically along with the sample size of natural FIA plots ($n = 364$, Table S6C; 39.6% mean class accuracy for natural forests and 78.9% for tree plantations).

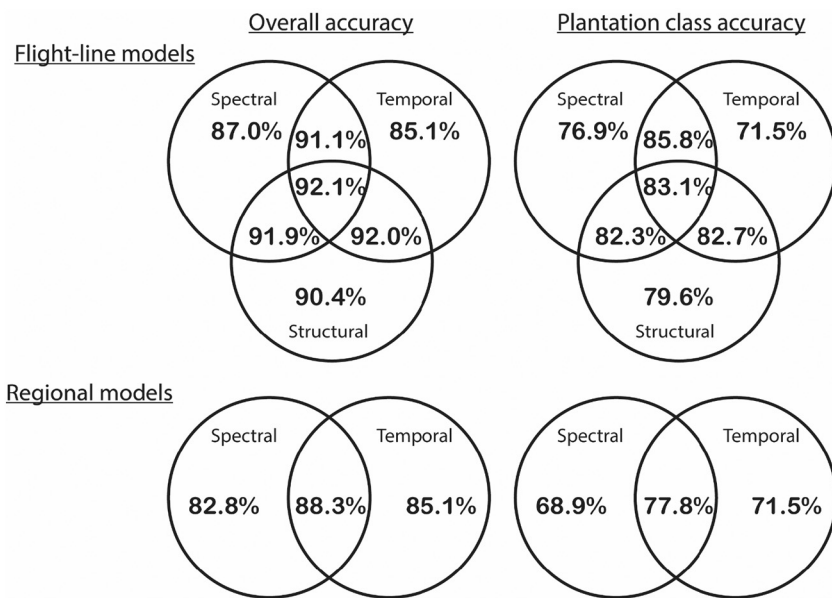


Fig. 3. Classification accuracy among models derived from the different data sources, and all possible data source combinations. Model accuracy was compared using the flight-line reference data (21 flight line segments) for both the flight-line classification models (all three data sources) and the regional classification models (only Landsat-derived data inputs).

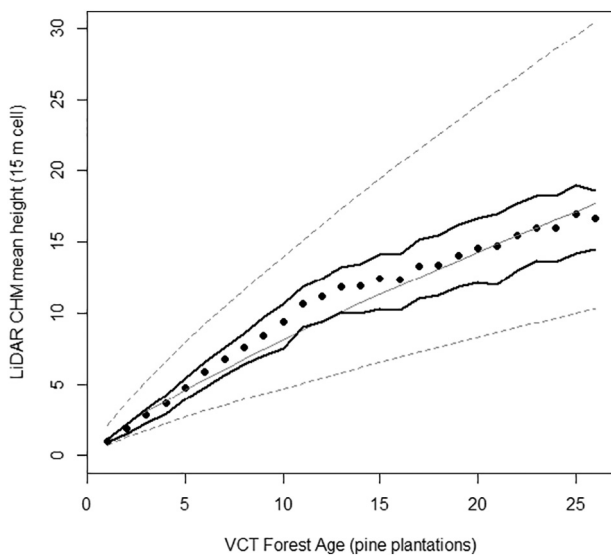


Fig. 4. Estimated forest age predicted tree plantation height well, with a median and range of variation that closely matched field plot estimates. Shown here is a regression of LiDAR tree height (mean of canopy height model in a 15 m cell) of tree plantations against estimated forest age derived from the Vegetation Change Tracker (VCT) dataset. Tree height data were filtered to biologically realistic growth rates to remove outliers resulting from post-harvest seed-tree retention, following Neigh et al. (2016). The black dots show the median height values, the black lines the first and third quartiles, the gray line the power law regression line prediction, and the dotted gray lines show the 95% confidence intervals on the regression.

3.3. Tree plantations in existing maps

The accuracy of plantation forest estimates from existing forest maps differed by 11–21% (mean class accuracy) from results using the multi-source classification approach in this study (Table 2). Based on reference data, the NLCD map had high errors of omission for pine plantations (Table 2); only 53% of the reference data for tree plantations was classified as evergreen forest in NLCD (Fig. S3), with 20% considered woody wetlands, 22% shrublands, and smaller proportions classified as mixed (2%) or deciduous forest (4%). By definition, re-growing pine would be categorized as a shrub class in NLCD (< 5 m in height), but the NLCD shrub class included both plantations and natural

Table 1

Regional map accuracy was high using two independent assessments, as shown in the confusion matrices for the regional classification (created using only Landsat-derived spectral and temporal data and filtered to a 2.5 ha minimum mapping unit). Post-stratified accuracy estimates come from a) independent FIA plot data and b) independent reference data derived from Google Earth imagery. The post-stratified error matrix is expressed in terms of estimated area proportions (see Table S6 for the count error matrix).

A) Regional map accuracy		FIA reference data				
Predicted	Natural forest	Nonforest	Tree plantations	Total	User Acc.	
Natural forest	0.37	0.03	0.04	0.45	82.8	
Open	0.01	0.37	0.01	0.39	95.0	
Tree plantations	0.04	0.00	0.12	0.16	75.8	
Total	0.42	0.41	0.17	1.00		Overall
Prod. Acc.	87.6	91.7	71.3			86.5
B) Regional map accuracy		Google Earth reference data				
Predicted	Natural forest	Nonforest	Tree plantations	Total	User Acc.	
Natural forest	0.42	0.00	0.03	0.45	93.2	
Open	0.01	0.37	0.01	0.39	94.9	
Tree plantations	0.02	0.003	0.14	0.16	85.7	
Total	0.45	0.37	0.18	1.0		Overall
Prod. Acc.	92.9	99.2	78.0			92.6

forests (Fig. S3) across a wide range of mean canopy heights (mean = 7.3 m, SD = 4.5 m; Fig. S4). This limited its utility in identifying young pine plantations, even in regions such as the southeast U.S. with few natural shrubland cover types. If the NLCD evergreen and shrub land cover classes were used together to estimate plantation extent in the flight-line reference data, they would omit 25% of the plantations and assign 26% of natural forests to the plantation category.

Similarly, the presence of pine plantations was poorly predicted by

Table 2

Existing forest map products have relatively poor accuracy predicting tree plantations and natural forests, based on flight-line reference data. Maps are compared using mean class accuracy, user's accuracy (100-error of commission), and producer's accuracy (100-error of omission). Forest map predictions (NLCD, VCT Forest Age, HGFC Forest Gain, and simple composite of the three, VCT-HGFC-NLCD) are compared to the best regional model (LSPEC-TEMP) and the filtered regional model (2.5 ha minimum mapping unit). The Supplementary materials details how tree plantation presence was predicted from prior forest maps.

Prediction inputs	Producer's accuracy		User's accuracy		Mean class accuracy	
	NF	TP	NF	TP	NF	TP
LSPEC-TEMP (filt)	88.4	82.2	90.9	90.1	89.7	86.2
LSPEC-TEMP	84.3	76.5	87.3	79.1	85.8	77.8
VCT-HGFC-NLCD	79.6	71.9	88.1	78.8	83.8	75.2
HGFC forest gain	91.0	45.2	73.9	84.4	82.5	64.8
VCT forest age	65.3	86.6	91.5	57.9	78.4	72.3
NLCD	71.3	84.2	92.7	64.8	82.0	74.5

map products tracking forest disturbance and regrowth (Table 2). VCT forest age was a poor predictor of plantations, with 42.1% commission error compared to flight-line reference data, as many forests < 25 years in age were natural forests, not plantations (Fig. S5). The HGFC was similarly inaccurate, with plantation omission error of 54.8%. Estimates of regrowth differed between VCT and HGFC (Fig. S5), underscoring the complexity of forest dynamics in the southeastern U.S. Finally, the simple composite NLCD-VCT-HGFC map fared the best among the existing forest maps, with producer's accuracies for forest types only ~5% lower than the multi-source map (Table 2).

3.4. Pine plantation dynamics

Using the best performing spectral-temporal model, industrial pine plantations cover an estimated $17.6 \pm 3\%$ of the southeastern ecoregion in 2011, or about 28.1% of the total forest area (Fig. 5). Individual patches of pine plantations ranged in size from 2.25 to 49,757 ha, with a mean patch size of 22 ± 161 ha. Mapped industrial forests had a mean age of 11.2 ± 9.8 years, with no apparent spatial trend in age, while most natural forests were > 25 years in age (pre-1984) (Fig. S6). Mapped industrial pine plantations comprised a larger fraction of the landscape in the southern half of the study region, from the coast to the interior (Figs. 5, 6a; trend surface model $p < 0.00001$, $r^2 = 0.20$).

Estimated spatial dynamics of plantation expansion, disturbance, and rotation age were not uniform across the region, and were characterized by rapid turnover and regrowth. From 1992 to 2011, pine plantations expanded into nonforest at a mean rate of 1.08% a year. Expansion was more common in the interior and southern portions of the study region (Fig. 6b; trend surface model $p < 0.00001$, $r^2 = 0.12$), with most new plantations adjacent to existing industrial forests (mean expansion distance = 145 m, expected random distance = 1086 m, $p < 0.0001$). By contrast, the area of stand-clearing disturbances of pine plantations largely mirrored the occurrence of pine plantations (Fig. 6c; trend surface model $p < 0.00001$, $r^2 = 0.06$). Disturbances were identified in 78% mapped pine plantations since 1985, with an estimated mean disturbance rate of 3.6% per year of plantations mapped in 2011. The area of stands disturbed at least twice during the Landsat record was also concentrated in the coastal southeast of the study region, with small hotspots of frequent disturbance (Fig. S7; trend surface model $p < 0.00001$, $r^2 = 0.08$). The rotation age of pine plantations had a distinct spatial pattern, decreasing to the southwest of the study area (Fig. 6d; trend surface model $p < 0.00001$,

$r^2 = 0.09$). The mean rotation age across the study area was 14.0 ± 3.1 years.

4. Discussion

4.1. Mapping pine plantations with structural, spectral, and temporal data

Industrial pine plantations can be accurately separated from natural forests using either structural information from airborne lidar or a combination of spectral and temporal Landsat metrics. Only structural metrics derived from small footprint lidar achieved > 90% classification accuracy in distinguishing forest types without other data sources. The combination of spectral and temporal Landsat metrics was more accurate than either source independently, and rivaled the accuracy of lidar-derived structural data in discriminating pine plantations. Importantly, combining information from more than one source of remote sensing data to map plantations led to improvements in classification accuracy over existing map products. Our findings demonstrate the potential to improve national and global map products of dynamic land cover types in human-dominated landscapes using multi-source remote sensing data. Multi-source regional maps revealed novel, spatially disaggregated patterns in plantation forest cover and dynamics, consistent with plot sampling across the southeastern U.S. but at finer temporal and spatial scales than can be achieved using inventory data.

Lidar provides novel information on forest structure that complements existing approaches to map forest cover and dynamics with passive optical remote sensing data. Both large and small footprint lidar have been successfully used to detect forest structure and disturbance across multiple ecosystems (e.g., Bright et al., 2012; Fagan and DeFries, 2009; Froking et al., 2009; Goetz et al., 2009). Where forest types may be more readily distinguishable based on structure rather than species, as in the case of native tree plantations, using lidar to map forest composition is a natural extension of previous work (Asner et al., 2008; Donoghue et al., 2007; Gopalakrishnan et al., 2015; Zhang et al., 2011). We found that simple lidar metrics played an important role in improving forest classification, including the standard deviation in return height, the lowest decile of LiDAR canopy height (p10), and fractional tree cover. The global extent of lidar data is growing, and lidar can be integrated with other structural information derived from stereoscopic high-resolution imagery or InSAR data (Neigh et al., 2016; Qi and Dubayah, 2016). In this study, more detailed metrics of forest structure (CHM and vertical profile variability) further improved discrimination of forest types. The upcoming launch of the Global Ecosystem Dynamics Investigation (GEDI) lidar to the international space station will provide a large sample of temperate and tropical forests (Qi and Dubayah, 2016). As we demonstrate, integrating lidar data with spectral and temporal data from Landsat, Sentinel-2, and other moderate resolution imagers offers great promise for large-scale assessments of managed forest landscapes.

Harvest or conifer dominance by themselves are not unique predictors of plantation forests, as forest management occurs in both pine plantations and natural mixed conifer/deciduous forests (Schroeder et al., 2014). Maps of forest regrowth (VCT, HGFC) did not distinguish plantation harvesting and regrowth from that of natural forests. Similarly, the generic NLCD classes assigned pine plantations (a land use) to multiple land cover classes (e.g., evergreen, shrub, and mixed forest cover in NLCD). Existing land cover products are not well suited to capture the diversity of vegetation physiognomies that comprise the cycle of plantation growth and harvest. These individual products were not specifically designed to monitor plantations, but their mapping of forest disturbance and type was quite informative when taken together. In the final regional decision tree model, integrating NLCD land cover data with data on the occurrence of regrowth set up broad classes that could be separated into natural and industrial forests by applying spectral thresholds to different forest ages. Conifer-dominated forests of different ages can have distinct but overlapping spectral signatures

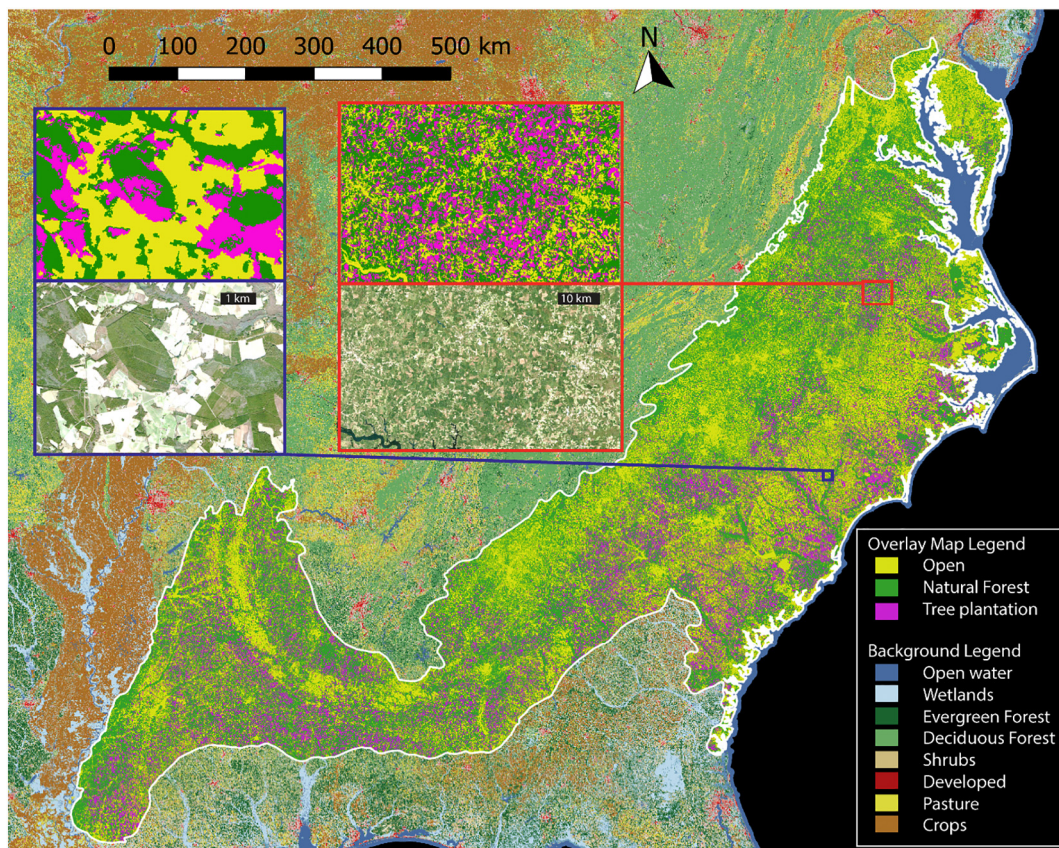


Fig. 5. The dominance of tree plantations as a land use in the study region is shown by the final classified map, created using the best regional model (LSPEC-TEMP, filtered). The classified map is overlaid on top of the NLCD map, with two insets that compare the 2011 map classification against recent high resolution imagery (Bing; winter 2015). Pine plantations appear as large dark green patches in the high-resolution imagery. (For interpretation of the references to colour in this figure legend, the reader is referred to the web version of this article.)

(Song et al., 2007), and industrial plantations had larger patch sizes than natural conifer patches in this study (and potentially distinct shapes; see Boschetti and Huo, 2016). The spectral-temporal classification results in this study indicate that integrating conifer cover derived from Landsat-derived seasonal phenology metrics with annual disturbance estimates could improve the discrimination of pine plantations from natural pine forests with less frequent disturbances. This computationally intensive approach has been pioneered by several groups (Brooks et al., 2014; Zhu et al., 2012).

This study capitalized on a relatively unique spectral signature that separated the target plantation species from other natural forest species; evergreen phenology of conifers. Where such spectral differences exist between native species, spectral data can be effectively and simply used to discriminate potential monocultures. Where spectral differences between plantation and natural forests are minimal, a combination of structural and temporal data could still be effective in identifying disturbance and regrowth cycles typical of short-rotation plantation management or even-aged canopy structure in plantations. Although the availability of lidar data provides limited spatial and temporal coverage, other remotely-sensed measures of forest structure from SAR (Reiche et al., 2016) and high-resolution stereo imagery (Neigh et al., 2016) cover large areas and time series of these measurements span a decade or more. As in many remote sensing studies, the complementary nature of independent remote sensing data types can provide multiple constraints on complex aspects of the Earth system. In this study, overall accuracy results clearly demonstrated the value of adding data types. However, not all combinations led to improved classifier performance with the CART decision tree algorithm, possibly due to correlated predictor combinations (Hayes et al., 2015).

4.2. Challenges with using multiple remote sensing products to map plantations

Despite the potential benefits for mapping native tree plantations, synchronizing multiple remote sensing products across space and time remains a challenge. Differences in the locations of disturbance and regrowth between the VCT and HGFC datasets were common, as were differences in forest cover predicted by the airborne lidar, NLCD, VCT, and HGFC datasets. Planted forests are a dynamic forest type with frequent disturbances, so differences in mere months between image acquisition dates may account for some of the discrepancies between the VCT and HGFC map products. The algorithms underlying current forest change products also differ in their sensitivity to forest management (Cohen et al., 2017).

Three additional temporal challenges also impact the maps of pine plantations developed in this study. First, the relatively short Landsat historical record (1985–2011) limited our ability to detect harvesting and regrowth patterns on plantations with longer management cycles. Although pine plantations > 26 years were spectrally distinct from natural forests, best practices for timber plantations in the southeastern U.S. recommend a rotation age of 25–35 years (Sohngren and Brown, 2008). Therefore, it is possible that the total area of older pine plantations in the southeastern U.S. was underestimated. Second, spectral and structural separability of plantation and natural forests differed as a function of stand age. The fate of young regrowth is particularly uncertain in the years following harvest (Fig. S6). Alternative management strategies for thinning or establishing more productive pine stands may also introduce confusion for older age classes. Third, a single-date map of tree plantations cannot detect historical conversion of natural forests to pine plantations or vice versa (“cryptic deforestation” sensu

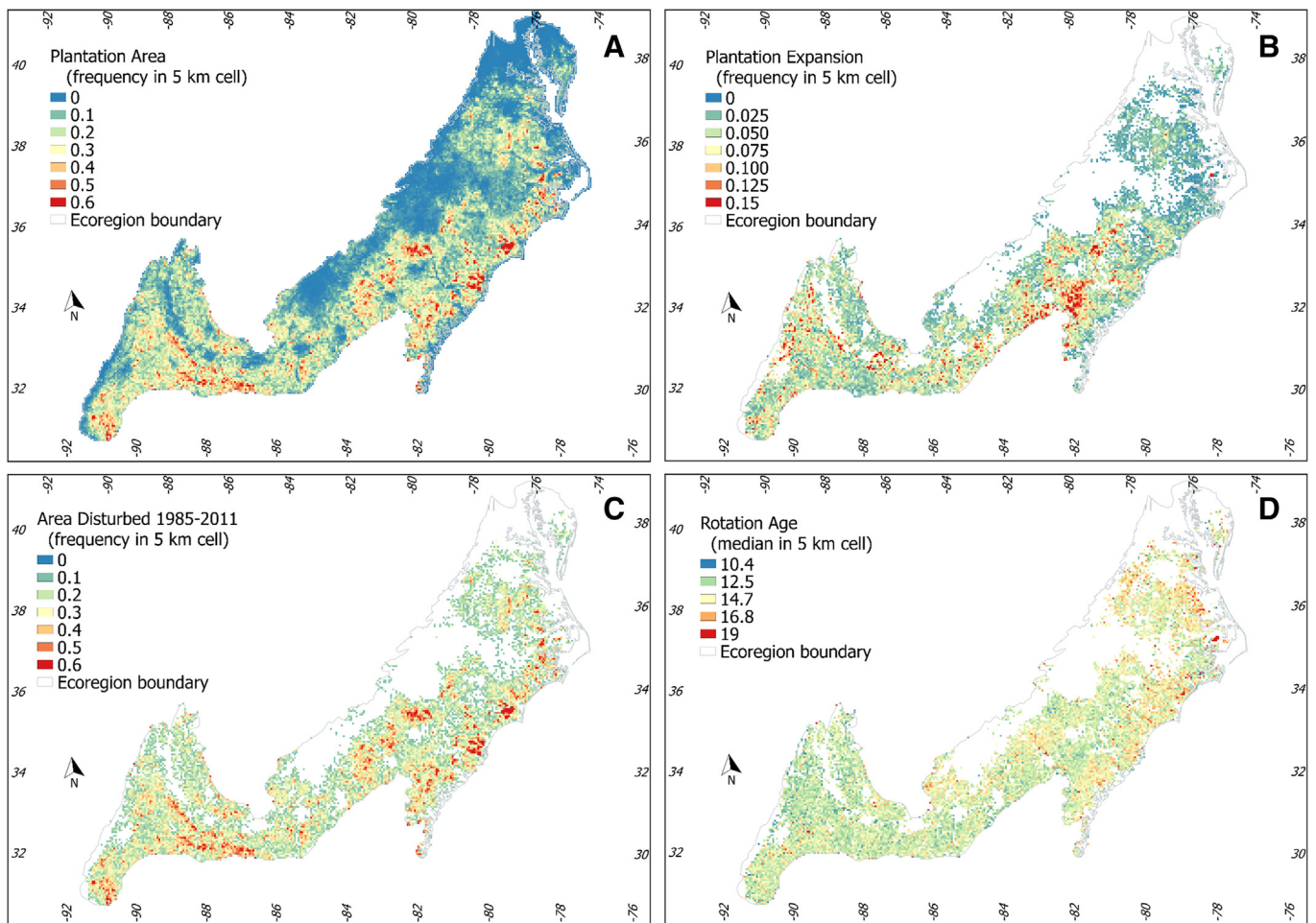


Fig. 6. Pine plantations across the study region in 2011 showed distinct patterns for A) estimated area, B) area of plantations that expanded into nonforest (1992–2011), C) area of plantations in 2011 disturbed at least once between 1985 and 2011, and D) plantation rotation age. Area was summarized as frequency of occurrence in 5 km grid cells, while rotation age was summarized as the median value in 5 km grid cells.

Puyravaud et al., 2010). The practice of replacing natural with planted forests is widespread in the region and quite important for regional biodiversity and carbon storage (Hanberry, 2013; Wear and Greis, 2013).

Harmonizing forest cover definitions between field and remote sensing studies may also improve the utility of satellite products for forest managers. For example, different definitions of plantations may partially explain the inconsistencies between FIA validation data and satellite-derived estimates of plantation forest cover in this study. FIA land use codes consider forest embedded in a nonforest matrix as nonforest (O'Connell et al., 2015), and the majority of nonforest commission error in this analysis resulted from forest elements embedded in other land uses (*unpublished data*; see also Johnson et al., 2015, 2014). Industrial pine plantations in this study were defined as managed, even-aged pine monocultures, which includes both artificially planted or seeded forests and semi-natural planted forests (SNPF) managed to increase the proportion of desirable species. Unlike the FAO, the FIA definition of planted forest excludes SNPF (Jürgensen et al., 2014; O'Connell et al., 2015). However even-aged pine monocultures resulting from intensively managed succession are common in the region (Wear and Greis, 2002), with seed tree silviculture followed by hardwood removal and thinning of pines. These management practices were directly observable in the high-resolution imagery time series used to develop the reference and validation data, yet SNPF are largely indistinguishable from planted forests after stand closure and thinning. Expanding the description of FIA stand origin to include a broad range of

forest management practices would better align FIA inventories with remotely-sensed estimates of plantation forests.

4.3. Distribution and dynamics of plantation forests

Regional maps of plantation forest cover were consistent with existing estimates of pine plantation extent, growth rates, and harvest dynamics, albeit with finer spatial detail. Pine plantations mapped in this study made up a slightly higher percentage (28.1%) of regional forest cover than previous, plot-based estimates for the larger southern or southeastern region as a whole (18.1–25%; Oswald et al., 2014; Wear and Greis, 2013, 2002; Zhang and Polyakov, 2010). The spatial distribution of mapped plantations were also in accordance with previous county-level maps of tree plantation cover (Wear and Greis, 2013; Zhang and Polyakov, 2010). However, the finer spatial scale of Landsat data identified hotspots not indicated in previous work, most notably the occurrence of linear bands of high plantation cover across the coastal Carolinas, interior Carolinas to Georgia, and central Alabama. Plantations were increasingly dominant in flatter southern and coastal regions, exceeding 70% of total cover in selected locations. Height and age relationships for plantations based on VCT forest age data and lidar in this study were quite similar to yield estimates from managed loblolly pine across the region (Devan and Burkhart, 1982; Diéguez-Aranda et al., 2006). Despite potential underestimation of stand age, as VCT considers both clear-cut harvest and thinning events as stand-clearing disturbances (Masek et al., 2013), VCT estimates of stand age

could be used in conjunction with lidar or stereo imagery (Neigh et al., 2016) to evaluate regional carbon dynamics in managed pine plantations.

Maps of plantation forests and harvest dynamics offer specific insights into regional forest management. Although estimated rates of stand disturbance (3.6%/year) and plantation expansion into nonforest (1.08%/year) were consistent with FIA plot data (3.1% and 1.10% per year respectively; Wear and Greis, 2002), our analysis revealed distinct spatial patterns for plantation expansion and overall plantation disturbance. The ability to disaggregate regional forest trends using spatially explicit estimates of plantation dynamics may uncover different underlying biophysical and socioeconomic drivers of plantation expansion and harvest (Wear and Greis, 2013, 2002; Zhang and Polyakov, 2010). For example, the estimated average rotation age of 14 years was concordant with regional plot data, which shows a peak in harvesting from 10 to 15 years (Coulston et al., 2015). This relatively short rotation may result from the mix of average harvest ages for timber (25–35 years; Sohngren and Brown, 2008) and pulp/biomass (10+ years; Wear and Greis, 2013). Rising prices for biofuels and wood pellets are projected to incentivize early harvesting (Abt et al., 2014; Abt and Abt, 2013; Coulston et al., 2015), and predicted spatial trends in demand for pulp and bioenergy production roughly correspond with the observed east-to-west decrease in rotation age in this study (Abt et al., 2014). In future work, it may be possible to combine high-resolution maps of plantation area and forest disturbances to track the impacts of changes in market demand and management on forest age and harvesting.

4.4. Broader implications

Mapping and monitoring of industrial pine monocultures is possible based on multi-source remote sensing of their distinct phenology, disturbance history, age-specific reflectance, and patch size. Mapping plantations with satellite imagery offers an opportunity to leverage periodic plot measurements of planted forests to generate spatially-explicit estimates of planted area (e.g., Schroeder et al., 2014). The growing extent of industrial pine plantations in the southeastern U.S. contributes to changes in future regional carbon sequestration, wood production, and habitat availability (Coulston et al., 2015; Masek and Collatz, 2006; Wear and Greis, 2013; Zhou et al., 2013). Given their regional significance, adding a tree plantation class to regional and national land cover maps (e.g., NLCD) would better capture the distinct influence of industrial forests in studies of land cover dynamics, biodiversity, and biogeochemical cycling. The integration of structural, spectral, and temporal data may also yield benefits for mapping other cover types in managed landscapes. Growing data availability from moderate resolution passive optical imagery and active radar and lidar sensors will support the routine use of data fusion approaches for regional and global-scale mapping efforts.

Declarations of interest

None.

Acknowledgements

Funding for this study was provided by a NASA Postdoctoral Program fellowship (M. Fagan) and NASA's Carbon Monitoring System and Carbon Cycle Science Programs.

Appendix A. Supplementary data

Supplementary data to this article can be found online at <https://doi.org/10.1016/j.rse.2018.07.007>.

References

- Abt, R.C., Abt, K.L., 2013. Potential impact of bioenergy demand on the sustainability of the southern forest resource. *J. Sustain. For.* 32, 175–194.
- Abt, K.L., Abt, R.C., Galik, C.S., Skog, K.E., 2014. Effect of Policies on Pellet Production and Forests in the U.S. South: A Technical Document Supporting the Forest Service Update of the 2010 RPA Assessment. Gen. Tech. Rep. SRS-202. U.S. Department of Agriculture Forest Service, Southern Research Station, Asheville, NC (33 pp.).
- Asner, G.P., Knapp, D.E., Kennedy-Bowdoin, T., Jones, M.O., Martin, R.E., Boardman, J., Hughes, R.F., 2008. Invasive species detection in Hawaiian rainforests using airborne imaging spectroscopy and LiDAR. *Remote Sens. Environ.* 112, 1942–1955. <https://doi.org/10.1016/j.rse.2007.11.016>.
- Banskota, A., Wynne, R.H., Kayastha, N., 2011. Improving within-genus tree species discrimination using the discrete wavelet transform applied to airborne hyperspectral data. *Int. J. Remote Sens.* 32, 3551–3563. <https://doi.org/10.1080/01431161003698302>.
- Blinn, C.E., Albaugh, T.J., Fox, T.R., Wynne, R.H., Stape, J.L., Rubilar, R.A., Allen, H.L., 2012. A method for estimating deciduous competition in pine stands using Landsat. *South. J. Appl. For.* 36, 71–78. <https://doi.org/10.5849/sjaf.10-034>.
- Boisvenue, C., Smiley, B.P., White, J.C., Kurz, W.A., Wulder, M.A., 2016. Integration of Landsat time series and field plots for forest productivity estimates in decision support models. *For. Ecol. Manag.* 376, 284–297. <https://doi.org/10.1016/j.foreco.2016.06.022>.
- Boschetti, L., Huo, L.Z., 2016. Forest disturbances, deforestation and timber harvest patterns in the Conterminous United States. In: AGU Fall Meeting Abstracts.
- Breiman, L., Friedman, J., Stone, C.J., Olshen, R.A., 1984. *Classification and Regression Trees*. CRC Press, Monterey, CA.
- Bright, B.C., Hicke, J.A., Hudak, A.T., 2012. Estimating aboveground carbon stocks of a forest affected by mountain pine beetle in Idaho using lidar and multispectral imagery. *Remote Sens. Environ.* 124, 270–281. <https://doi.org/10.1016/j.rse.2012.05.016>.
- Brockerhoff, E.G., Jactel, H., Parrotta, J.A., Quine, C.P., Sayer, J., 2008. Plantation forests and biodiversity: oxymoron or opportunity? *Biodivers. Conserv.* 17, 925–951. <https://doi.org/10.1007/s10531-008-9380-x>.
- Brooks, E.B., Wynne, R.H., Thomas, V.A., Blinn, C.E., Coulston, J.W., 2014. On-the-fly massively multitemporal change detection using statistical quality control charts and Landsat data. *IEEE Trans. Geosci. Remote Sens.* 52, 3316–3332. <https://doi.org/10.1109/TGRS.2013.2272545>.
- Chen, B., Li, X., Xiao, X., Zhao, B., Dong, J., Kou, W., Qin, Y., Yang, C., Wu, Z., Sun, R., Lan, G., Xie, G., 2016. Mapping tropical forests and deciduous rubber plantations in Hainan Island, China by integrating PALSAR 25-m and multi-temporal Landsat images. *Int. J. Appl. Earth Obs. Geoinf.* 50, 117–130. <https://doi.org/10.1016/j.jag.2016.03.011>.
- Cohen, W.B., Yang, Z., Stehman, S.V., Schroeder, T.A., Bell, D.M., Masek, J.G., Huang, C., Meigs, G.W., 2016. Forest disturbance across the conterminous United States from 1985–2012: the emerging dominance of forest decline. *For. Ecol. Manag.* 360, 242–252. <https://doi.org/10.1016/j.foreco.2015.10.002>.
- Cohen, W., Healey, S., Yang, Z., Stehman, S., Brewer, C., Brooks, E., Gorelick, N., Huang, C., Hughes, M., Kennedy, R., Loveland, T., Moisen, G., Schroeder, T., Vogelmann, J., Woodcock, C., Yang, L., Zhu, Z., 2017. How similar are forest disturbance maps derived from different Landsat time series algorithms? *Forests* 8, 98. <https://doi.org/10.3390/f8040098>.
- Cook, B.D., Corp, L.A., Nelson, R.F., Morton, D.C., Middleton, E.M., McCorkel, J.T., Masek, J.G., Ranson, K.J., Ly, V., Montesano, P.M., 2013. NASA Goddard's LiDAR, Hyperspectral and Thermal (G-LiHT) airborne imager. *Remote Sens.* 5.
- Coulston, J.W., Wear, D.N., Vose, J.M., 2015. Complex forest dynamics indicate potential for slowing carbon accumulation in the southeastern United States. *Sci. Rep.* 5, 8002. <https://doi.org/10.1038/srep08002>.
- Czaplewski, R.L., 2010. *Complex Sample Survey Estimation in Static State-Space*. Gen. Tech. Rep. RMRS-239. (Fort Collins, CO).
- Danson, F.M., Curran, P.J., 1993. Factors affecting the remotely sensed response of coniferous forest plantations. *Remote Sens. Environ.* 43, 55–65. [https://doi.org/10.1016/0034-4257\(93\)90064-5](https://doi.org/10.1016/0034-4257(93)90064-5).
- Devan, J.S., Burkhart, H.E., 1982. Polymorphic site index equations for loblolly pine based on a segmented polynomial differential model. *For. Sci.* 28, 544–555.
- Diéguez-Aranda, U., Burkhart, H.E., Amateis, R.L., 2006. Dynamic site model for loblolly pine (*Pinus taeda* L.) plantations in the United States. *For. Sci.* 52, 262–272.
- Dong, J., Xiao, X., Chen, B., Torbick, N., Jin, C., Zhang, G., Biradar, C., 2013. Mapping deciduous rubber plantations through integration of PALSAR and multi-temporal Landsat imagery. *Remote Sens. Environ.* 134, 392–402. <https://doi.org/10.1016/j.rse.2013.03.014>.
- Donoghue, D.N.M., Watt, P.J., Cox, N.J., Wilson, J., 2007. Remote sensing of species mixtures in conifer plantations using LiDAR height and intensity data. *Remote Sens. Environ.* 110, 509–522. <https://doi.org/10.1016/j.rse.2007.02.032>.
- Drummond, M.A., Stier, M.P., Auch, M.P., Taylor, J.L., Griffith, G.E., Riegler, J.L., Hester, D.J., Soular, C.E., McBeth, J.L., 2015. Assessing landscape change and processes of recurrence, replacement, and recovery in the Southeastern Coastal Plains, USA. *Environ. Manag.* 56, 1252–1271. <https://doi.org/10.1007/s00267-015-0574-1>.
- Fagan, M.E., DeFries, R.S., 2009. *Measurement and Monitoring of the World's Forests: A Review and Summary of Technical Capability, 2009–2015. The World's Forests: Design and Implementation of Effective Measurement and Monitoring Resources for the Future (RFF)*. Washington, DC.
- Fagan, M.E., Defries, R.S., Sesnie, S.E., Arroyo-Mora, J.P., Soto, C., Singh, A., Townsend, P.A., Chazdon, R.L., 2015. Mapping species composition of forests and tree plantations in Northeastern Costa Rica with an integration of hyperspectral and

- multitemporal Landsat imagery. *Remote Sens.* 7, 5660. <https://doi.org/10.3390/rs70505660>.
- FAO, 2015a. Global Forest Resources Assessment 2015. Food and Agriculture Organization of the United Nations, Rome, Italy.
- FAO, 2015b. Global Forest Resources Assessment 2015. (Rome).
- Frolking, S., Palace, M.W., Clark, D.B., Chambers, J.Q., Shugart, H.H., Hurtt, G.C., 2009. Forest disturbance and recovery: a general review in the context of spaceborne remote sensing of impacts on aboveground biomass and canopy structure. *J. Geophys. Res.* 114 (doi:G00e0210.1029/2008jg000911).
- Goetz, S.J., Baccini, A., Laporte, N.T., Johns, T., Walker, W., Kellndorfer, J., Houghton, R. a, Sun, M., 2009. Mapping and monitoring carbon stocks with satellite observations: a comparison of methods. *Carbon Balance Manag.* 4, 2. <https://doi.org/10.1186/1750-0680-4-2>.
- Gopalakrishnan, R., Thomas, V.A., Coulston, J.W., Wynne, R.H., 2015. Prediction of canopy heights over a large region using heterogeneous Lidar datasets: efficacy and challenges. *Remote Sens.* 7, 11036–11060. <https://doi.org/10.3390/rs70911036>.
- Gutiérrez-Vélez, V.H., DeFries, R., 2013. Annual multi-resolution detection of land cover conversion to oil palm in the Peruvian Amazon. *Remote Sens. Environ.* 129, 154–167. <https://doi.org/10.1016/j.rse.2012.10.033>.
- Hanberry, B.B., 2013. Changing eastern broadleaf, southern mixed, and northern mixed forest ecosystems of the eastern United States. *For. Ecol. Manag.* 306, 171–178. <https://doi.org/10.1016/j.foreco.2013.06.040>.
- Hansen, M.C., Potapov, P.V., Moore, R., Hancher, M., Turubanova, S.A., Tyukavina, A., Thau, D., Stehman, S.V., Goetz, S.J., Loveland, T.R., Kommareddy, A., Egorov, A., Chini, L., Justice, C.O., Townshend, J.R.G., 2013. High-resolution global maps of 21st-century forest cover change. *Science* 342, 850–853. <https://doi.org/10.1126/science.1244693>.
- Harris, N.L., Hagen, S.C., Saatchi, S.S., Pearson, T.R.H., Woodall, C.W., Domke, G.M., Braswell, B.H., Walters, B.F., Brown, S., Salas, W., Fore, A., Yu, Y., 2016. Attribution of net carbon change by disturbance type across forest lands of the conterminous United States. *Carbon Balance Manag.* 11, 24. <https://doi.org/10.1186/s13021-016-0066-5>.
- Hayes, T., Usami, S., Jacobucci, R., McArdle, J.J., 2015. Using Classification and Regression Trees (CART) and random forests to analyze attrition: results from two simulations. *Psychol. Aging* 30, 911–929. <https://doi.org/10.1037/pag0000046>.
- Huang, C., Goward, S.N., Masek, J.G., Thomas, N., Zhu, Z., Vogelmann, J.E., 2010. An automated approach for reconstructing recent forest disturbance history using dense Landsat time series stacks. *Remote Sens. Environ.* 114, 183–198. <https://doi.org/10.1016/j.rse.2009.08.017>.
- Homer, C., Dewitz, J., Yang, L., Jin, S., Danielson, P., Xian, G., Coulston, J., Herold, N., Wickham, J., Megown, K., 2015. Completion of the 2011 National Land Cover Database for the conterminous United States—representing a decade of land cover change information. *Photogramm. Eng. Remote Sens.* 81, 345–354.
- Jin, S., Yang, L., Danielson, P., Homer, C., Fry, J., Xian, G., 2013. A comprehensive change detection method for updating the National Land Cover Database to circa 2011. *Remote Sens. Environ.* 132, 159–175. <https://doi.org/10.1016/j.rse.2013.01.012>.
- Johnson, K.D., Birdsey, R., Finley, A.O., Swatantran, A., Dubayah, R., Wayson, C., Riemann, R., 2014. Integrating forest inventory and analysis data into a LIDAR-based carbon monitoring system. *Carbon Balance Manag.* 9, 3. <https://doi.org/10.1186/1750-0680-9-3>.
- Johnson, K.D., Birdsey, R., Cole, J., Swatantran, A., O'Neil-Dunne, J., Dubayah, R., Lister, A., 2015. Integrating LIDAR and forest inventories to fill the trees outside forests data gap. *Environ. Monit. Assess.* 187, 623. <https://doi.org/10.1007/s10661-015-4839-1>.
- Joshi, N., Baumann, M., Ehammer, A., Fensholt, R., Grogan, K., Hostert, P., Jepsen, M., Kuemmerle, T., Meyfroidt, P., Mitchard, E., Reiche, J., Ryan, C., Waske, B., 2016. A review of the application of optical and radar remote sensing data fusion to land use mapping and monitoring. *Remote Sens.* 8, 70. <https://doi.org/10.3390/rs8010070>.
- Jürgensen, C., Kollert, W., Lebedys, A., 2014. Assessment of Industrial Roundwood Production from Planted Forests. Planted Forests and Trees Working Paper Series, No. FP/48/E The Food and Agricultural Organization of the United Nations (FAO), Rome.
- le Maire, G., Dupuy, S., Nouvellon, Y., Loos, R.A., Hakamada, R., 2014. Mapping short-rotation plantations at regional scale using MODIS time series: case of eucalypt plantations in Brazil. *Remote Sens. Environ.* 152, 136–149. <https://doi.org/10.1016/j.rse.2014.05.015>.
- Masek, J.G., Collatz, G.J., 2006. Estimating forest carbon fluxes in a disturbed southeastern landscape: Integration of remote sensing, forest inventory, and biogeochemical modeling. *J. Geophys. Res. Biogeosci.* 111 <https://doi.org/10.1029/2005JG000062>. (n/a-n/a).
- Masek, J.G., Goward, S.N., Kennedy, R.E., Cohen, W.B., Moisen, G.G., Schleeweis, K., Huang, C., 2013. United States forest disturbance trends observed using Landsat time series. *Ecosystems* 16, 1087–1104. <https://doi.org/10.1007/s10021-013-9669-9>.
- Neigh, C.S.R., Masek, J.G., Nickeson, J.E., 2013. High-resolution satellite data open for government research. *EOS Trans. Am. Geophys. Union* 94, 121–123. <https://doi.org/10.1002/2013EO130002>.
- Neigh, C.S.R., Masek, J.G., Bourget, P., Rishmawi, K., Zhao, F., Huang, C., Cook, B.D., Nelson, R.F., 2016. Regional rates of young US forest growth estimated from annual Landsat disturbance history and IKONOS stereo imagery. *Remote Sens. Environ.* 173, 282–293. <https://doi.org/10.1016/j.rse.2015.09.007>.
- Nelson, R., Margolis, H., Montesano, P., Sun, G., Cook, B., Corp, L., Andersen, H.-E., deJong, B., Pellat, F.P., Fickel, T., Kauffman, J., Prisley, S., 2017. Lidar-based estimates of aboveground biomass in the continental US and Mexico using ground, airborne, and satellite observations. *Remote Sens. Environ.* 188, 127–140. <https://doi.org/10.1016/j.rse.2016.10.038>.
- O'Connell, B.M., LaPoint, E.B., Turner, J.A., Ridley, T., Pugh, S.A., Wilson, A.M., Waddell, K.L., Conkling, B.L., 2015. The Forest Inventory and Analysis Database: Database Description and User Guide Version 6.0.2 for Phase 2. (Washington, DC).
- Olofsson, P., Foody, G.M., Stehman, S.V., Woodcock, C.E., 2013. Making better use of accuracy data in land change studies: estimating accuracy and area and quantifying uncertainty using stratified estimation. *Remote Sens. Environ.* 129, 122–131. <https://doi.org/10.1016/j.rse.2012.10.031>.
- Olson, D.M., Dinerstein, E., Wikramanayake, E.D., Burgess, N.D., Powell, G.V.N., Underwood, E.C., D'Amico, J.A., Itoua, I., Strand, H.E., Morrison, J.C., 2001. Terrestrial ecoregions of the world: a new map of life on earth: a new global map of terrestrial ecoregions provides an innovative tool for conserving biodiversity. *Bioscience* 51, 933–938.
- Oswalt, S.N., Smith, W.B., Miles, P.D., Pugh, S.A., 2014. Forest Resources of the United States, 2012: A Technical Document Supporting the Forest Service 2010 Update of the RPA Assessment. Gen. Tech. Rep. WO-91. (Washington, DC).
- Pan, Y., Chen, J.M., Birdsey, R., McCullough, K., He, L., Deng, F., 2011. Age structure and disturbance legacy of North American forests. *Biogeosciences* 8, 715.
- Payn, T., Carnus, J.-M., Freer-Smith, P., Kimberley, M., Kollert, W., Liu, S., Orazio, C., Rodriguez, L., Silva, L.N., Wingfield, M.J., 2015. Changes in planted forests and future global implications. *For. Ecol. Manag.* 352, 57–67. <https://doi.org/10.1016/j.foreco.2015.06.021>.
- Petersen, R., Goldman, E.D., Harris, N., Sargent, S., Aksenov, D., Manisha, A., Esipova, E., Shevade, V., Loboda, T., Kuksina, N., 2016. Mapping Tree Plantations With Multispectral Imagery: Preliminary Results for Seven Tropical Countries. World Resour. Institute, Washington, DC.
- Pfennigbauer, M., Ullrich, A., 2010. Improving quality of laser scanning data acquisition through calibrated amplitude and pulse deviation measurement. In: SPIE Proceedings. Laser Radar Technology and Applications 7684.
- Popescu, S.C., Wynne, R.H., Scrivani, J.A., 2004. Fusion of small-footprint lidar and multispectral data to estimate plot-level volume and biomass in deciduous and pine forests in Virginia, USA. *For. Sci.* 50, 551–565.
- Puyravaud, J.-P., Davidar, P., Laurance, W.F., 2010. Cryptic destruction of India's native forests. *Conserv. Lett.* 3, 390–394. <https://doi.org/10.1111/j.1755-263X.2010.00141.x>.
- Qi, W., Dubayah, R.O., 2016. Combining Tandem-X InSAR and simulated GEDI lidar observations for forest structure mapping. *Remote Sens. Environ.* 187, 253–266.
- Qin, Y., Xiao, X., Dong, J., Zhang, G., Roy, P.S., Joshi, P.K., Gilani, H., Murthy, M.S.R., Jin, C., Wang, J., 2016. Mapping forests in monsoon Asia with ALOS PALSAR 50-m mosaic images and MODIS imagery in 2010. *Sci. Rep.* 6, 20880.
- R Core Team, 2013. R: A Language and Environment for Statistical Computing.
- Reiche, J., Lucas, R., Mitchell, A.L., Verbesselt, J., Hoekman, D.H., Haarpaintner, J., Kellndorfer, J.M., Rosenqvist, A., Lehmann, E.A., Woodcock, C.E., Seifert, F.M., Herold, M., 2016. Combining satellite data for better tropical forest monitoring. *Nat. Clim. Chang.* 6, 120–122.
- Ruefenacht, B., Finco, M.V., Nelson, M.D., Czaplowski, R., Helmer, E.H., Blackard, J.A., Holden, G.R., Lister, A.J., Salajanu, D., Weyeremann, D., 2008. Conterminous US and Alaska forest type mapping using forest inventory and analysis data. *Photogramm. Eng. Remote Sens.* 74, 1379–1388.
- Sabatia, C.O., Burkhart, H.E., 2014. Predicting site index of plantation loblolly pine from biophysical variables. *For. Ecol. Manag.* 326, 142–156. <https://doi.org/10.1016/j.foreco.2014.04.019>.
- Schleeweis, K., Goward, S.N., Huang, C., Masek, J.G., Moisen, G., Kennedy, R.E., Thomas, N.E., 2013. Regional dynamics of forest canopy change and underlying causal processes in the contiguous US. *J. Geophys. Res. Biogeosci.* 118, 1035–1053. <https://doi.org/10.1002/jgrg.20076>.
- Schroeder, T.A., Healey, S.P., Moisen, G.G., Frescino, T.S., Cohen, W.B., Huang, C., Kennedy, R.E., Yang, Z., 2014. Improving estimates of forest disturbance by combining observations from Landsat time series with U.S. Forest Service Forest Inventory and Analysis data. *Remote Sens. Environ.* 154, 61–73. <https://doi.org/10.1016/j.rse.2014.08.005>.
- Shamsoddini, A., Trinder, J.C., Turner, R., 2013. Pine plantation structure mapping using WorldView-2 multispectral image. *Int. J. Remote Sens.* 34, 3986–4007. <https://doi.org/10.1080/01431161.2013.772308>.
- Smith, J.E., Heath, L.S., Skog, K.E., Birdsey, R.A., 2006. Methods for Calculating Forest Ecosystem and Harvested Carbon With Standard Estimates for Forest Types of the United States. Gen. Tech. Rep. NE-343. (Newtown Square, PA).
- Sohngren, B., Brown, S., 2008. Extending timber rotations: carbon and cost implications. *Clim. Pol.* 8, 435–451. <https://doi.org/10.3763/cpol.2007.0396>.
- Song, C., Schroeder, T.A., Cohen, W.B., 2007. Predicting temperate conifer forest successional stage distributions with multitemporal Landsat Thematic Mapper imagery. *Remote Sens. Environ.* 106, 228–237. <https://doi.org/10.1016/j.rse.2006.08.008>.
- Therneau, T., Atkinson, B., Ripley, B., 2015. rpart: Recursive Partitioning and Regression Trees.
- Torbick, N., Ledoux, L., Salas, W., Zhao, M., 2016. Regional mapping of plantation extent using multisensor imagery. *Remote Sens.* 8.
- van Aardt, J.A.N., Norris-Rogers, M., 2008. Spectral-age interactions in managed, even-aged Eucalyptus plantations: application of discriminant analysis and classification and regression trees approaches to hyperspectral data. *Int. J. Remote Sens.* 29, 1841–1845. <https://doi.org/10.1080/01431160701874546>.
- Van Aardt, J.A.N., Wynne, R.H., 2007. Examining pine spectral separability using hyperspectral data from an airborne sensor: an extension of field-based results. *Int. J. Remote Sens.* 28, 431–436. <https://doi.org/10.1080/01431160500444772>.
- Wear, D.N., Greis, J.G., 2002. Southern Forest Resource Assessment - Technical Report. Gen. Tech. Rep. SRS-53. (Asheville, NC).
- Wear, D.N., Greis, J.G., 2013. The Southern Forest Futures Project: Technical Report. Gen. Tech. Rep. SRS-GTR-178. (Asheville, NC).
- Wear, D.N., Prestemon, J.P., Foster, M.O., 2016. US forest products in the global economy. *J. For.* 114, 483–493. <https://doi.org/10.5849/jof.15-091>.

- Williams, C.A., Collatz, G.J., Masek, J., Huang, C., Goward, S.N., 2014. Impacts of disturbance history on forest carbon stocks and fluxes: merging satellite disturbance mapping with forest inventory data in a carbon cycle model framework. *Remote Sens. Environ.* 151, 57–71. <https://doi.org/10.1016/j.rse.2013.10.034>.
- Xian, G., Homer, C., Fry, J., 2009. Updating the 2001 National Land Cover Database land cover classification to 2006 by using Landsat imagery change detection methods. *Remote Sens. Environ.* 113, 1133–1147. <https://doi.org/10.1016/j.rse.2009.02.004>.
- Yeo, I.-Y., Huang, C., 2013. Revisiting the forest transition theory with historical records and geospatial data: a case study from Mississippi (USA). *Land Use Policy* 32, 1–13. <https://doi.org/10.1016/j.landusepol.2012.09.017>.
- Zhang, D., Polyakov, M., 2010. The geographical distribution of plantation forests and land resources potentially available for pine plantations in the U.S. South. *Biomass Bioenergy* 34, 1643–1654. <https://doi.org/10.1016/j.biombioe.2010.05.006>.
- Zhang, Z., Liu, X., Peterson, J., Wright, W., 2011. Cool temperate rainforest and adjacent forests classification using airborne LiDAR data. *Area* 43, 438–448. <https://doi.org/10.1111/j.1475-4762.2011.01035.x>.
- Zhao, F., Huang, C., Goward, S.N., Schleeweis, K., Rishmawi, K., Lindsey, M.A., Denning, E., Keddell, L., Cohen, W.B., Yang, Z., 2018. Development of Landsat-based annual US forest disturbance history maps (1986–2010) in support of the North American Carbon Program (NACP). *Remote Sens. Environ.* 209, 312–326.
- Zhou, D., Liu, S., Oeding, J., Zhao, S., 2013. Forest Cutting and Impacts on Carbon in the Eastern United States. 3. pp. 3547.
- Zhu, Z., Woodcock, C.E., Olofsson, P., 2012. Continuous monitoring of forest disturbance using all available Landsat imagery. *Remote Sens. Environ.* 122, 75–91.